

High-transition-temperature superconductivity in the absence of the magnetic-resonance mode

J. Hwang¹, T. Timusk¹ and G.D. Gu^{2*}

¹Department of Physics and Astronomy, McMaster University, Hamilton, ON L8S 4M1, Canada

²Department of Physics, Brookhaven National Laboratory, Upton, New York 11973-5000, USA

(Dated: October 31, 2018)

PACS numbers: 74.25.Gz, 74.62.Dh, 74.72.Hs

The fundamental mechanism that gives rise to high-transition-temperature (high- T_c) superconductivity in the copper oxide materials has been debated since the discovery of the phenomenon. Recent work has focussed on a sharp 'kink' in the kinetic energy spectra of the electrons as a possible signature of the force that creates the superconducting state [1, 2, 3, 4, 5, 6, 7, 8, 9, 10, 11, 12, 13, 14]. The kink has been related to a magnetic resonance [13, 15, 16, 17] and also to phonons [18]. Here we report that infrared spectra of $\text{Bi}_2\text{Sr}_2\text{CaCu}_2\text{O}_{8+\delta}$ (Bi-2212) show that this sharp feature can be separated from a broad background and, interestingly, weakens with doping before disappearing completely at a critical doping level of 0.23 holes per copper atom. Superconductivity is still strong in terms of the transition temperature ($T_c \approx 55$ K), so our results rule out both the magnetic resonance peak and phonons as the principal cause of high- T_c superconductivity. The broad background, on the other hand, is a universal property of the copper oxygen plane and a good candidate for the 'glue' that binds the electrons.

We investigated the Bi-2212 material systematically as a function of doping, including highly overdoped Bi-2212 (see Methods). To better display the sharp 'kink', we do not show the optical conductivity but focus our attention on a related quantity, the optical single particle self-energy, $\Sigma^{op}(\omega)$ (see Methods). In Fig. 1a-d we plot the imaginary part of this quantity which is simply the scattering rate of the charge carriers. At high frequencies the scattering rate varies linearly with frequency: this is called the marginal Fermi liquid (MFL) behavior [19]. We note that the overall scattering rate decreases as the doping increases and that there is a sharp depression in $1/\tau(\omega)$ below 700 cm^{-1} at low temperatures, with an overshoot in the superconducting state. This sharp onset of scattering has been in general attributed to the interaction of the charge carriers with a bosonic mode and more recently to the 41 meV neutron resonance [7, 13, 14]. In the real part of the optical self-energy, plotted in panels 1e-h, we note a sharp peak around 700 cm^{-1} , which tracks the depressions in $1/\tau(\omega)$ in both frequency and amplitude. One very interesting property of the peak

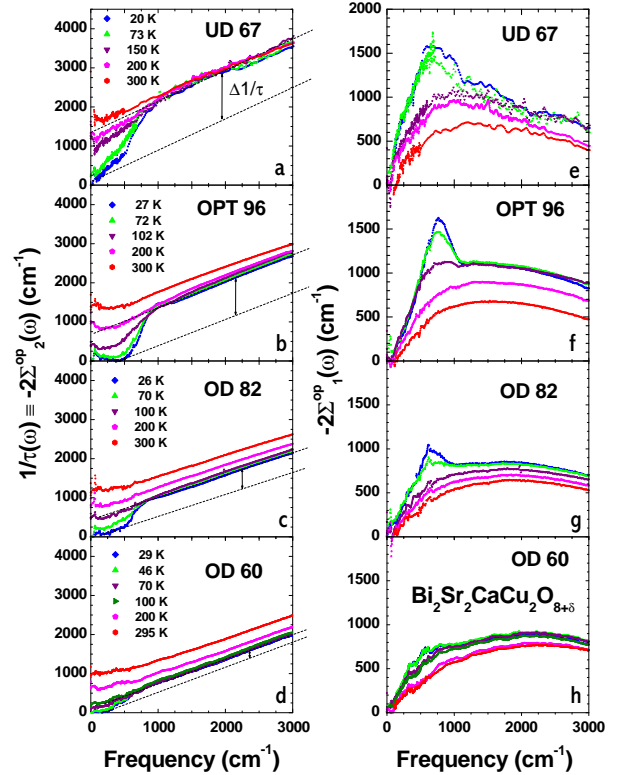


FIG. 1: The optical single-particle self-energy of $\text{Bi}_2\text{Sr}_2\text{CaCu}_2\text{O}_{8+\delta}$. a-d, The doping and temperature dependent optical scattering rate, $1/\tau(\omega)$ for four representative doping levels. a, $T_c = 67$ K (underdoped); b, 96 K (optimal); ac, 82 K (overdoped); d, 60 K (overdoped). e-h, The real part of the optical self-energy, $-2\Sigma_1^{op}(\omega)$. The slope of $-\Sigma_1^{op}(\omega)$ near $\omega = 0$, is closely related to the coupling constant or the mass enhancement factor, and also decreases as the doping increases. This is consistent with other studies [6, 24]. We note the weakening of the feature at 700 cm^{-1} in both sets of curves as the doping level increases.

in the self-energy is its doping and temperature dependence: the peak gets weaker as the doping level and the temperature increase. We will call the peak the 'optical resonance mode'. The resonance peak in the self-energy spectrum can clearly be resolved from the broader background of MFL scattering.

The optical self-energy is closely related to the quasi-particle self-energy $\Sigma^{qp}(\omega)$, which can be measured in ARPES experiments although there are important dif-

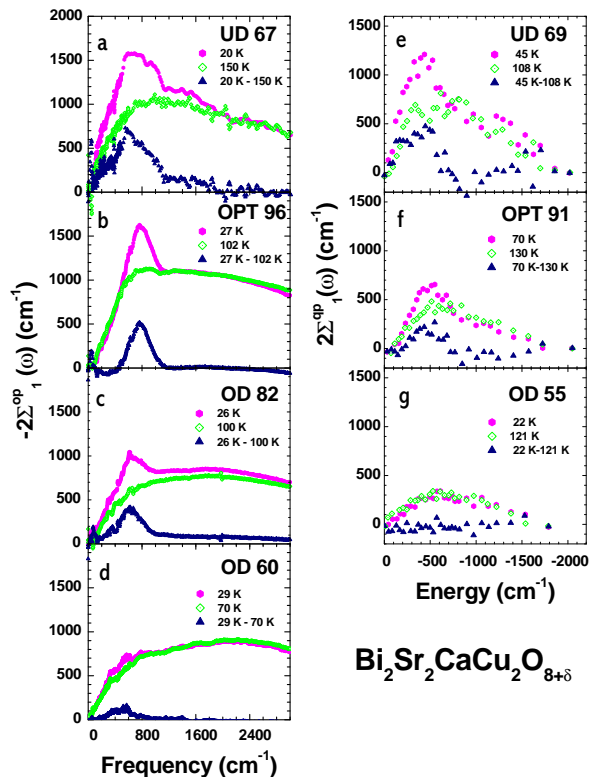


FIG. 2: Comparison of the self energy measured with infrared and angle-resolved photoemission for Bi-2212. a-d, The real part of the optical self-energies, $-2\Sigma_1^{op}(\omega)$ of the normal and superconducting phases for a series of crystals with different doping levels determined by FTIR spectroscopy, as well as the difference between normal and superconducting state curves. a, $T_c = 67$ K (underdoped); b, 96 K (optimal); ac, 82 K (overdoped); d, 60 K (overdoped). e-g, The real part of the self-energies, $-2\Sigma_1^{qp}(\omega)$ from ARPES measurements of ref. 6. e, $T_c = 69$ K (underdoped); f, $T_c = 91$ K (optimal); g, $T_c = 55$ K (overdoped). Although the absolute magnitudes and frequencies differ for the two data sets, the overall qualitative features are closely correlated when one allows for the higher noise level and lower resolution of the photoemission data.

ferences in the two quantities [20, 21, 22]. In Fig. 2 we show a comparison of the optical self-energy from our data and the ARPES self-energy at two temperatures: one in the normal state and the other the superconducting state. We see that although the qualitative features are very similar, the magnitudes and the frequency values of the various features differ considerably, as expected from theory. Part of the difference can be attributed to the uncertainty in locating the unrenormalized base line in the ARPES analysis. As noted in ref. 6, a peak in $\Sigma_1^{qp}(\omega)$ can be clearly separated from the broad continuum and is closely correlated with the neutron resonance mode. The lower noise level and the higher resolution of our optical data demonstrate a clear doping dependent trend – the amplitude of the resonance peak weakens with doping in the overdoped region and disappears com-

pletely at a doping level where the superconductivity is still large enough to show $T_c \approx 55$ K, as shown in Fig. 2g. Thus, at this doping level we have superconductivity without the resonance peak, and whereas the peak may contribute to the condensation energy [16, 23] and the superconducting gap at lower doping levels, it cannot be the main cause of high- T_c superconductivity.

In Fig. 3 we investigate further the disappearance of the optical resonance mode as a function of doping. In Fig. 3a we plot the amplitude of the resonance mode in the real part of the optical self-energy, which decreases uniformly with doping and appears to extrapolate to zero at a doping level $p = 0.23$ ($T_c \approx 55$ K). The center frequency of the mode (Fig. 3b) is proportional to the transition temperature ($\Omega_{res}^{op} \approx 8.0k_B T_c$) and reaches a maximum at the optimally doped phase for both FTIR and ARPES, which is consistent with other studies [4]. In Fig. 3c we show the contribution of the resonance mode to the imaginary part of the self-energy as a function of doping, both directly and normalized as a percentage of the total scattering rate at 3000 cm^{-1} (see Methods). This is done to divide out the overall decrease of the coupling of the charge carriers to the bosonic fluctuations that occurs with increased doping [6, 24].

We do not have detailed data on the amplitude of the mode as a function of temperature. In the region of $p = 0.19$ the mode appears at the superconducting transition temperature of 80 K along with the neutron mode [3, 4]. The error in the critical doping value cannot be found from optical data alone because we were not able to obtain a sample with sufficient overdoping. The ARPES data of ref. 6 for their $T_c = 55$ K sample shows no resonance, so we can use this as an upper limit and our own 60 K sample as a lower limit, giving $p = 0.225 \pm 0.010$ for the value of the critical doping point.

While it is clear from our results that the amplitude of the coupling of the optical resonance mode to charge carriers extrapolates to zero at a critical doping of $p = 0.23$, we are not able to determine the behavior of the center frequency of the resonance mode at the critical doping point. The center frequency appears to drop below the parabolic trend, shown as the dashed curve in Fig. 3b. According to theory, the frequency of the ARPES resonance (Ω_{res}^{qp}) is roughly the sum of the gap (Δ) and the frequency of the neutron mode (Ω) [13] (we note that in optics $\Omega_{res}^{op} = 2\Delta + \Omega$).

We remark here on the relationship between our work and the proposal of Lanzara *et al.* [18] that the sharp kink seen in angle-resolved photoemission is due to phonons. With our higher resolution and lower noise level we are able to separate the sharp peak from the overall broad background. The broad background can be seen in the spectra of all high- T_c superconductors and seems to represent a universal property of the copper oxide plane. But it cannot be due to phonons, because its spectral weight extends beyond the cut-off frequency of the phonon spec-

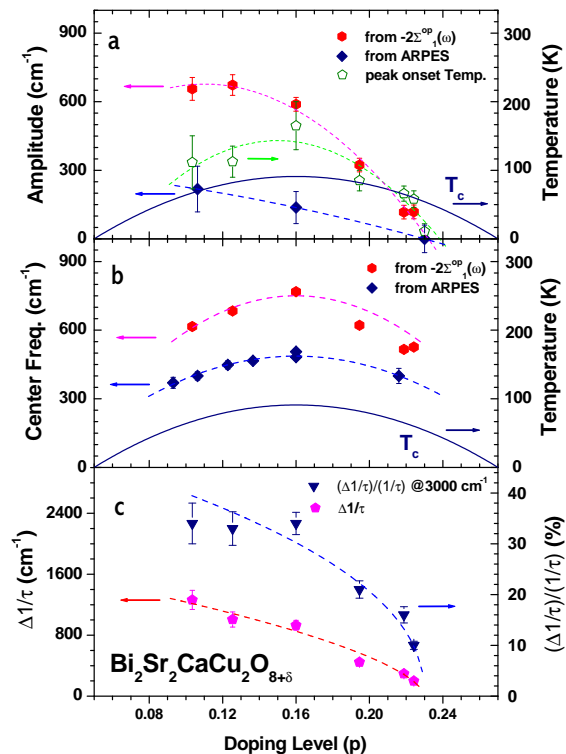


FIG. 3: Doping-dependent properties of the optical resonance mode. See the Methods section for detail descriptions. a, Amplitudes; b, center frequencies. The solid curve is $T_c(p)$ and the two dashed curves are parabolic fits, $5.6k_B T_c$ for ARPES and $8.0k_B T_c$ for FTIR. c, the quantity $\Delta 1/\tau$ (see Fig. 1 a-d), the contribution of the resonance mode to the scattering rate, as a function of doping, and the same quantity normalized to the scattering rate at 3000 cm^{-1} . All the data point to the disappearance of the mode at a critical doping level of $p = 0.23$.

trum [22]. The sharp structure, on the other hand, has all the characteristics of the magnetic resonance: it makes its appearance at the superconducting T_c in overdoped copper oxides and slightly above T_c in the underdoped copper oxides. We have also shown that it vanishes completely at a high doping level inside the superconducting dome. None of this is expected for phonons which should be present at all temperatures and doping levels.

The disappearance of the resonance mode may be related to the possible vanishing of the pseudogap and the existence of a quantum critical point [25, 26]. Recent data [27] suggests that the critical doping level for the disappearance of the pseudogap in c-axis transport may be higher than $p = 0.22$ at least in Bi-2212. The pseudogap has less influence than the resonance mode on ab-plane properties as shown by work on the anisotropy of dc transport [28]. Also on theoretical grounds, a gap in the fluctuation spectrum will not give the upward step in the scattering rate that we observe [7]. The disappearance of the resonance mode has been predicted to occur near

the $p = 0.22$ doping level within the magnetic exciton picture [9, 10]. Our analysis of the optical self-energy, which allows us to isolate the resonance peak from the universal broad background in the single-particle self-energy for Bi-2212, should work for other copper oxides and gives us a direct tool for examining the spectrum of excitations responsible for pairing in high- T_c superconductors.

Methods

Experiments and sample preparations

We used Fourier-transform infrared (FTIR) spectroscopy to obtain the reflectance data [29] of floating-zone-grown single-twinned crystals of Bi-2212. The highly overdoped samples were made by annealing the as-grown crystals at high temperature, $T > 500 \text{ }^\circ\text{C}$, in 3000 bar liquid oxygen in sealed containers. We present new data on one optimally doped Bi-2212 ($T_c = 96 \text{ K}$), and three highly overdoped samples ($T_c = 82 \text{ K}$, $T_c = 65 \text{ K}$, and $T_c = 60 \text{ K}$). The four new samples are bulk superconductors with London penetration depths of 2,065 Å, 1,638 Å, 1,481 Å and 1,375 Å, respectively. The optimally doped sample has been doped with a small amount of Y to yield a relatively well-ordered system [30]. To cover a wide range of doping levels we also used data from previously measured underdoped Bi-2212 crystals [12].

The optical single particle self-energy, $\Sigma^{op}(\omega)$

The optical conductivity was determined by Kramers-Kronig analysis [29] and we present our data within the framework of the extended Drude model, where the complex optical conductivity can be written as $\sigma(\omega) = -i\omega(\epsilon(\omega) - \epsilon_H)/4\pi = -i\omega_p^2/[4\pi(2\Sigma^{op}(\omega) - \omega)]$, where ϵ_H is the dielectric constant at a high frequency ($\sim 2eV$) for each doping level (note that there is doping dependence in ϵ_H), ω_p is the plasma frequency and $\Sigma^{op}(\omega) = \Sigma_1^{op}(\omega) + i\Sigma_2^{op}(\omega)$ is the optical single-particle self-energy. In terms of more familiar quantities $\Sigma_1^{op}(\omega) \equiv \omega(1 - m^*/m)/2$, where m^*/m is the mass renormalization, and $\Sigma_2^{op}(\omega) \equiv -1/(2\tau(\omega))$, where τ is the carrier lifetime. We determine the doping-dependent plasma frequency from the absorption spectra in the near-infrared region [24].

Doping dependence of the optical resonance mode in $\Sigma^{op}(\omega)$

We used the parabolic approximation to obtain the doping levels from the transition temperature, T_c , with the slope of the infrared reflectance as an additional test of the doping level [24]. The amplitude and center frequency of the optical resonance mode are obtained from $-2\Sigma_1^{op}(\omega)$ data by a least-squares fit of the peak to a Lorentzian line shape (see Fig. 3a and b). To estimate the strength of the interaction of the resonance mode with the carriers from $1/\tau(\omega) \equiv -2\Sigma_2^{op}(\omega)$, we draw a dashed line, parallel to the high frequency trend, from the onset point of substantial scattering. The difference between this line and the actual high frequency scattering, $\Delta 1/\tau$ is our estimate of the contribution of the sharp

mode to the scattering. It exhibits a doping dependence that is suggestive of mean-field behavior (dashed curve) with a critical point at $p = 0.23$. (see Fig. 1a-d and Fig. 3c). We estimate the doping dependence of the onset temperature of the resonance mode from both FTIR and ARPES data. We have drawn the points as follows: the upper error-limit temperature where there is no resonance. The lower-limit temperature is where we first see the resonance. The resonance onset temperature is the average of the upper and lower limits (see Fig. 3a).

* Electronic address: timusk@mcmaster.ca

- [1] Rossat-Mignod, J. *et al.* Neutron scattering study of the $\text{YBa}_2\text{Cu}_3\text{O}_{6+x}$ system. *Physica C* **185-189**, 86-92 (1991).
- [2] Mook, H. A. *et al.* Spin fluctuations in $\text{YBa}_2\text{Cu}_3\text{O}_{6.6}$. *Nature (London)* **395**, 580-582 (1998).
- [3] Fong, H. F. *et al.* Neutron scattering from magnetic excitations in $\text{Bi}_2\text{Sr}_2\text{CaCu}_2\text{O}_{8+\delta}$. *Nature (London)* **398**, 588-591 (1999).
- [4] He, H. *et al.* Resonant spin excitation in an overdoped high temperature superconductor. *Phys. Rev. Lett.* **86**, 1610-1613 (2001).
- [5] Kaminski A. *et al.* Renormalization of spectral line shape and dispersion below T_c in $\text{Bi}_2\text{Sr}_2\text{CaCu}_2\text{O}_{8+\delta}$. *Phys. Rev. Lett.* **86**, 1070-1073 (2001).
- [6] Johnson, P. D. *et al.* Doping and temperature dependence of the mass enhancement observed in the cuprate $\text{Bi}_2\text{Sr}_2\text{CaCu}_2\text{O}_{8+\delta}$. *Phys. Rev. Lett.* **87**, 177007/1-4 (2001).
- [7] Norman, M.R. & Ding, H. Collective modes and the superconducting-state spectral function of $\text{Bi}_2\text{Sr}_2\text{CaCu}_2\text{O}_{8+x}$. *Phys. Rev. B* **57**, R11089-11092 (1998).
- [8] Campuzano, J.C. *et al.* Electronic spectra and their relation to the (π, π) collective mode in high- T_c superconductors. *Phys. Rev. Lett.* **83**, 3709-3712 (1999).
- [9] Abanov, Ar. *et al.* A relation between the resonance neutron peak and ARPES data in cuprates. *Phys. Rev. Lett.* **83**, 1652-1655 (1999).
- [10] Zasadzinski, J. F. *et al.* Correlation of tunneling spectra in $\text{Bi}_2\text{Sr}_2\text{CaCu}_2\text{O}_{8+\delta}$ with the resonance spin excitation. *Phys. Rev. Lett.* **87**, 067005/1-4 (2001).
- [11] Thomas, G.A. *et al.* $\text{Ba}_2\text{YCu}_3\text{O}_{7-d}$: Electrodynamics of crystals with high reflectivity. *Phys. Rev. Lett.* **61**, 1313-1316 (1988).
- [12] Puchkov, A. V. *et al.* Evolution of the pseudogap state of high- T_c superconductors with doping. *Phys. Rev. Lett.* **77**, 3212-3215 (1996).
- [13] Carbotte, J. P. *et al.* Coupling strength of charge carriers to spin fluctuations in high-temperature superconductors. *Nature (London)* **401**, 354-356 (1999).
- [14] Munzar, D., Bernhard, C. & Cardona, M. Possible relationship between the peak in magnetic susceptibility and the in-plane far infrared conductivity of YBCO. *Physica C* **317-318**, 547-549 (1999).
- [15] Dai, Pengcheng *et al.* Resonance as a measure of pairing correlations in the high- T_c superconductor $\text{YBa}_2\text{Cu}_3\text{O}_{6.6}$. *Nature (London)* **406**, 965-968, (2000).
- [16] Demler, E. & Zhang, Z.C. Quantitative test of a microscopic mechanism of high-temperature superconductivity. *Nature (London)* **396**, 733-735 (1998).
- [17] Scalapino, D. J. The cuprate pairing mechanism. *Science* **284**, 1282-1283 (1999).
- [18] Lanzara, A. *et al.* Evidence for ubiquitous strong electron-phonon coupling in high-temperature superconductors. *Nature (London)* **412**, 510-514, (2001).
- [19] Varma, C. M. *et al.* Phenomenology of the normal state of Cu-O high-temperature superconductors. *Phys. Rev. Lett.* **63**, 1996-1999 (1989).
- [20] Kaminski A. *et al.* Quasiparticles in the superconducting state of $\text{Bi}_2\text{Sr}_2\text{CaCu}_2\text{O}_{8+\delta}$. *Phys. Rev. Lett.* **84**, 1788-1791 (2000).
- [21] Millis, A.J. & Drew, H.D. Quasiparticles in high temperature superconductors: consistency of angle resolved photoemission and optical conductivity. preprint: *cond-mat/0303018* (2003).
- [22] Schachinger, E., Tu, J.J. & Carbotte, J.P. Angle-resolved photoemission spectroscopy and optical renormalizations: phonons or spin fluctuations. *Phys. Rev. B* **67**, 214508/1-17, (2003).
- [23] Dai, Pengcheng *et al.* The magnetic excitation spectrum and thermodynamics of high- T_c superconductors. *Science* **284**, 1344-1347 (1999).
- [24] Hwang, J. *et al.* Marginal Fermi liquid analysis of 300 K reflectance of $\text{Bi}_2\text{Sr}_2\text{CaCu}_2\text{O}_{8+\delta}$. *cond-mat/0306250* (2003).
- [25] Chakravarty, S. *et al.* Hidden order in the cuprates. *Phys. Rev. B* **63**, 094503/1-10, (2001).
- [26] Loram, J.W. *et al.* The condensation energy and pseudogap energy scale of $\text{Bi}_2\text{212}$ from electronic specific heat. *Physica C* **341-348**, 831-834 (2000).
- [27] Shibauchi, T. *et al.* Closing the pseudogap by Zeeman splitting in $\text{Bi}_2\text{Sr}_2\text{CaCu}_2\text{O}_{8+y}$ at high magnetic fields. *Phys. Rev. Lett.* **86**, 5763-5766 (2001).
- [28] Takenaka, K., Mizuhashi, K., Takagi, H & Uchida, S. Interplane charge transport in $\text{YBa}_2\text{Cu}_3\text{O}_{7-y}$: Spin gap effect on in-plane and out-of-plane resistivity. *Phys. Rev. B* **50**, 6534-6537 (1994).
- [29] Homes, C. C. *et al.* Technique for measuring the reflectance of irregular, submillimeter-sized samples. *Appl. Optics.* **32**, 2976-2983 (1993).
- [30] H. Eisaki *et al.* Effect of chemical inhomogeneity in the bismuth-based copper oxide superconductors. to appear in *Phys. Rev. B* (preprint: *cond-mat/0312429*).

Acknowledgments

This work has been supported by the Canadian Natural Science and Engineering Research Council and the Canadian Institute of Advanced Research. We thank H. Eisaki and M. Greven for supplying us with several crystals. Their work at Stanford University was supported by the Department of Energy's Office of Basic Sciences, Division of Materials Science. The work at Brookhaven was supported in part by the the Department of Energy. We thank D.N. Basov, J.P. Carbotte, G.M. Luke and M.R. Norman for helpful discussions.